Letter

Impact of a plasma on the relaxation of black holes

Enrico Cannizzaro,[1,2] Thomas F. M. Spieksma,[2] Vitor Cardoso,[2,3,4] and Taishi Ikeda[2]

[1]*Dipartimento di Fisica, "Sapienza" Università di Roma and Sezione INFN Roma1, Piazzale Aldo Moro 5, 00185, Roma, Italy*

[2]*Niels Bohr International Academy, Niels Bohr Institute, Blegdamsvej 17, 2100 Copenhagen, Denmark*

[3]*CENTRA, Departamento de Física, Instituto Superior Técnico—IST, Universidade de Lisboa—UL, Avenida Rovisco Pais 1, 1049 Lisboa, Portugal*

[4]*Yukawa Institute for Theoretical Physics, Kyoto University, Kyoto 606-8502, Japan*

(Received 10 January 2024; accepted 11 June 2024; published 8 July 2024)

Our Universe is permeated with interstellar plasma, which prevents propagation of low-frequency electromagnetic waves. Here, we show that two dramatic consequences arise out of such suppression; (i) if plasma permeates the light ring of a black hole, electromagnetic modes are screened entirely from the gravitational-wave signal, changing the black hole spectroscopy paradigm; (ii) if a near vacuum cavity is formed close to a charged black hole, as expected for near equal-mass mergers, ringdown "echoes" are excited. The amplitude of such echoes decays slowly and could thus serve as a silver bullet for plasmas near charged black holes.

DOI: 10.1103/PhysRevD.110.L021302

Introduction. The ability to detect gravitational waves (GWs) opened new horizons to advance our understanding of the Universe [1–4]. GWs probe gravity in the strong-field, dynamical regime [5–10], they probe environments of compact objects [11–15], and illuminate the "dark" Universe [6,7,16–19]. Together with black holes (BHs), GWs hold an exciting potential to search for new interactions or physics. A particularly intriguing possibility concerns charge. Significant amounts of electromagnetic (EM) charge are not expected to survive long for accreting systems (due to selective accretion, Hawking radiation or pair production [20–22]), but exceptions exist. A fraction of the primordial BHs produced in the early universe can carry a large amount of charge, suppressing Hawking radiation and potentially allowing for electric or color-charged BHs to survive to our days [23,24]. Additionally, BH mergers might be accompanied by strong magnetic fields pushing surrounding plasma to large radii, and preventing neutralization processes. Beyond the realm of Standard Model physics, BHs could be charged in a variety of different models, by circumventing in different ways discharge mechanisms. These models include millicharged dark matter or hidden vector fields, constructed to be viable cold dark matter candidates [22,25–43]. Finally, some BH mimickers are globally neutral while possessing a non-vanishing dipole moment, thus emitting EM radiation. Examples include topological solitons in string-theory fuzzballs scenarios [44,45].

Charge constraints via GW dephasing in the inspiral phase of two compact objects, or via BH spectroscopy assume implicitly that photons propagate freely from source to observer [22,39,41,42]. But the Universe is filled with matter. Even if dilute, the interstellar plasma prevents the propagation of EM waves with frequencies smaller than the plasma frequency, which effectively behaves as an effective mass [46]:

$$\omega_{\rm p} = \sqrt{\frac{e^2 n_{\rm e}}{\epsilon_0 m_{\rm e}}} \sim 1.8 \times 10^3 \left(\frac{n_{\rm e}}{10^{-3}\ {\rm cm}^{-3}}\right)^{1/2} {\rm rad\,s}^{-1}, \quad (1)$$

where $n_{\rm e}$ is the electron number density in the plasma, whereas $m_{\rm e}$ and e are the electron mass and charge, respectively, and ϵ_0 is the vacuum permeability.

The emission of GWs and EMs during mergers of compact, charged objects is a coupled phenomenon. Hence, the BH *gravitational* spectrum contains EM-driven modes [47,48]. But if EM modes are unable to propagate, their impact on GW generation and propagation could be important, affecting spectroscopy tests to an unknown degree. Motivated by recent progress [46,49,50], the purpose of this *Letter* is to close the gap, by showing from first principles that (i) EM waves are indeed screened by plasma, which filters out EM-led modes from GWs and (ii) in certain plasma-depleted environments, GW echoes are triggered, serving as a clear observational signature of plasmas surrounding charged BHs. A schematic illustration of our setup is shown in Fig. 1.

We adopt the mostly positive metric signature and use geometrized units in which $G = c = 1$ and Gaussian units for the Maxwell equations. In general, we denote dimensionless quantities with a bar, such as the charge $\bar{Q} = Q/M$ or the plasma frequency $\bar{\omega}_{\rm p}^{(\rm c)} = M\omega_{\rm p}^{(\rm c)}$.

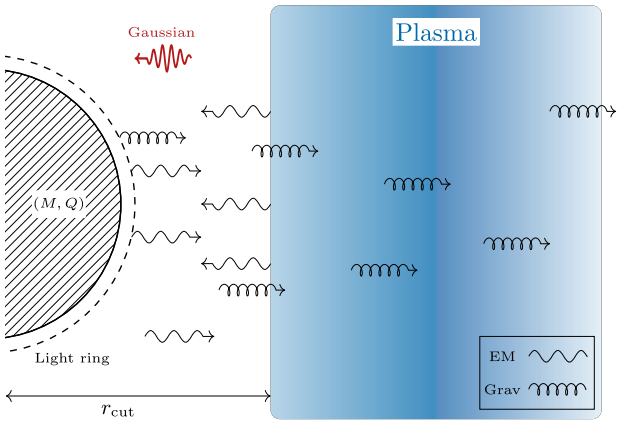

FIG. 1. Schematic illustration of our setup: a charged BH surrounded by plasma is stimulated by external processes (an initial gaussian wave packet), emitting electromagnetic and gravitational radiation. While GWs are able to travel through the plasma to distant observers, low frequency EM waves are not. Instead they excite further GWs, echoes of the original burst.

Setup. We consider a stationary system of charged, gravitating particles, i.e., an "Einstein cluster," surrounding a charged BH [12,13,51–53]. The key idea behind the model is to perform an angular average over particles in circular motion in all possible orientations, which is equivalent to considering an anisotropic, static fluid with a nonvanishing tangential pressure. Focusing on a fluid consisting of electrons, the stress-energy tensor reads[1]

$$T^{\rm p}_{\mu\nu} = (\rho + P_{\rm t}) v_\mu v_\nu + P_{\rm t}(g_{\mu\nu} - r_\mu r_\nu), \tag{2}$$

where $\rho = n_{\rm e} m_{\rm e}$ is the energy density of the fluid, v^μ the four-velocity, $P_{\rm t}$ the tangential pressure, $g_{\mu\nu}$ the metric of the underlying spacetime and r^μ a unit vector in the radial direction.

We then consider Einstein-Maxwell theory in the presence of this fluid. The relevant field equations are

$$G_{\mu\nu} = 8\pi(T^{\rm EM}_{\mu\nu} + T^{\rm p}_{\mu\nu}), \qquad \nabla_\nu F^{\mu\nu} = j^\mu, \tag{3}$$

where $G_{\mu\nu}$ and $F_{\mu\nu}$ are the Einstein and Maxwell tensor, respectively, $j^\mu = e n_{\rm e} v^\mu$ the plasma current and $T^{\rm EM}_{\mu\nu}$ is the stress-energy tensor for the EM sector:

$$T^{\rm EM}_{\mu\nu} = \frac{1}{4\pi}\left(g^{\rho\sigma} F_{\rho\mu} F_{\sigma\nu} - \frac{1}{4} g_{\mu\nu} F_{\rho\sigma} F^{\rho\sigma}\right). \tag{4}$$

Finally, to close the system, the momentum and continuity equation of the charged fluid are needed, which are derived from the conservation of the stress-energy tensors and the current,

$$\nabla^\nu T^{\rm p}_{\mu\nu} = e n_{\rm e} F_{\mu\nu} v^\nu, \qquad \nabla_\mu (n_{\rm e} v^\mu) = 0. \tag{5}$$

In the following, we ignore backreaction of the fluid in the Einstein and Maxwell equations as source terms are suppressed by the large charge-to-mass ratio of the electron, and energy densities of astrophysical fluids are small. In addition, astrophysical plasmas typically include ions, which induce a current with the opposite sign in the Maxwell equations and can be considered a stationary, neutralizing background [49,50,54,55]. Accordingly, one obtains the Reissner-Nordström (RN) solution from Eq. (3), describing a spherically symmetric, charged BH:

$$\begin{aligned} {\rm d}s^2 &= -f {\rm d}t^2 + f^{-1} {\rm d}r^2 + r^2 {\rm d}\Omega^2, \\ \text{with} \quad f &= 1 - \frac{2M}{r} + \frac{Q^2}{r^2}, \end{aligned} \tag{6}$$

where M and Q are BH mass and charge, respectively, and ${\rm d}\Omega^2$ is the metric on the 2-sphere. The event horizon is at $r_+ = M + \sqrt{M^2 - Q^2}$ and the light ring at $r_{\rm LR} = 3M/2 + \sqrt{9M^2 - 8Q^2}/2$. We will assume a nonrelativistic fluid, i.e., $P_{\rm t} \ll \rho$, such that (2) reduces to $T^{\rm p}_{\mu\nu} \approx \rho v_\mu v_\nu + P_{\rm t}(g_{\mu\nu} - r_\mu r_\nu)$, and the left-hand side of the momentum equation (5) resembles the nonrelativistic Euler equation. Solving the momentum equation (5) then yields the tangential pressure

$$P_{\rm t} = -\frac{n_{\rm e}\left(eQr\sqrt{f} + (Q^2 - Mr) m_{\rm e}\right)}{Q^2 - 3Mr + 2r^2}. \tag{7}$$

For the nonrelativistic assumption $P_{\rm t} \ll \rho = n_{\rm e} m_{\rm e}$ to hold, we must have either $Q/M < m_{\rm e}/e$ or $r \gg M$. Given the large charge-to-mass ratio of electrons ($e/m_{\rm e} \approx 10^{22}$), the former condition is only satisfied for extremely weakly charged BHs. Nevertheless, a number of effects can affect this outcome, such as magnetic fields, the formation of a cavity in the plasma due to mergers [56–62] or the partial screening of the BH charge by plasma over a Debye length [53,63]. In the following, we consider high values of Q as a proxy to model these scenarios, which are too complicated to be included in a self-consistent way. Moreover, for millicharged dark matter, the charge-to-mass ratio of the particles can be arbitrarily small.

Considering the full momentum equation allows us to study the relativistic regime as well. As detailed in the Supplemental Material [64], this regime generates similar results, albeit with a largely suppressed effective mass. Interestingly, this suppression can be understood as a form of strong-field *transparency* for relativistic plasmas, induced by the background charge Q [46,65]. Upon tuning the plasma density, we thus expect the same phenomenology to hold. Furthermore, at large distances the transparency effect vanishes, yielding the standard effective mass.

[1]The following discussion also applies to millicharged dark matter. For clarity purposes, we focus on electrons.

Consider now the linearization of the field equations (3) around the RN geometry, the background fields and fluid variables. Perturbations can then be decomposed in two sectors—*axial* (or odd) and *polar* (or even)—depending on their behavior under parity transformations. These two sectors decouple in spherically symmetric geometries (see Supplemental Material [64]) [66–72].

The axial sector is completely determined by two functions, a Moncrief-like "master gravitational" variable Ψ [73–75] and a "master EM" variable u_4, which obey a coupled set of second order, partial differential wavelike equations,

$$\hat{\mathcal{L}}\Psi = \left(\frac{4Q^4}{r^6}+\frac{Q^2\left(-14M+r(4+\lambda)\right)}{r^5} + \left(1-\frac{2M}{r}\right)\left[\frac{\lambda}{r^2}-\frac{6M}{r^3}\right]\right)\Psi - \frac{8Qf}{r^3\lambda}u_4,$$
$$\hat{\mathcal{L}}u_4 = f\left(\omega_{\rm p}^2+\frac{\lambda}{r^2}+\frac{4Q^2}{r^4}\right)u_4 - \frac{(\ell-1)\lambda(\ell+2)Qf}{2r^3}\Psi, \quad (8)$$

where $\lambda=\ell(\ell+1)$, $\hat{\mathcal{L}}=\partial^2/\partial r_*^2-\partial^2/\partial t^2$ and the tortoise coordinate is defined as $\mathrm{d}r_*/\mathrm{d}r=f^{-1}$. Note that in the limit $Q\to 0$, the equations decouple: the first one reduces to the Regge-Wheeler equation while the second one coincides with the axial mode of an EM field in Schwarzschild in the presence of plasma [49].

The polar sector is more intricate, with EM and fluid perturbations being coupled. As detailed in the Supplemental Material [64], at large radii and neglecting metric fluctuations, we recover the dispersion relation $(\omega^2-k^2-\omega_{\rm p}^2)\delta F_{12}=0$, where k is the wave vector in Fourier space and δF_{12} the perturbed Maxwell tensor. The plasma frequency thus acts as an effective mass for the propagating degree of freedom in the polar sector. As the dynamics emerging in the axial sector are precisely contingent upon this fact, we expect the phenomenology to be similar [49,50] and we hereafter focus only on the axial sector.

Initial conditions, plasma profile, and numerical procedure. We evolve the wavelike equations (8) in time with a two-step Lax-Wendroff algorithm that uses second-order finite differences [76], following earlier work [76–80]. Our grid is uniformly spaced in tortoise coordinates r_*, with the boundaries placed sufficiently far away such that boundary effects cannot have an impact on the evolution of the system at the extraction radius. Our code shows second-order convergence (see Supplemental Material [64]).

We consider a plasma profile truncated at a radius $r_{\rm cut}$, smoothened by a sigmoidlike function:

$$\omega_{\rm p}=\omega_{\rm p}^{(\rm c)}\frac{1}{1+e^{-(r-r_{\rm cut})/d}}. \quad (9)$$

Here, $\omega_{\rm p}^{(\rm c)}$ is the (constant) amplitude of the plasma barrier and d determines how "sharp" the cut is. We choose $d=M$, but we verified that the results are not sensitive to this parameter.[2] Profile (9) allows us to consider two distinct scenarios; (i) plasmas that "permeate" the light ring ($r_{\rm cut}<r_{\rm LR}$), hence possibly affecting the *generation* of quasinormal modes (QNMs) and (ii) plasmas localized away from the BH ($r_{\rm cut}\gg r_{\rm LR}$), affecting at most the *propagation* of the signal. We consider the initial conditions $\Psi(0,r)=\Psi_0, u_4(0,r)=u_{40}$ with [46]

$$(\Psi_0,u_{40})=(A_{\rm g},A_{\rm EM})\exp\left[-\frac{(r_*-r_0)^2}{2\sigma^2}-i\Omega_0 r_*\right],$$
$$\partial_t\Psi_0=-i\Omega_0\Psi_0, \qquad \partial_t u_{40}=-i\Omega_0 u_{40}, \quad (10)$$

where $(A_{\rm g},A_{\rm EM})=(1,0),(0,1),(1,1)$ for $\mathrm{ID_g}, \mathrm{ID_{EM}}$ and $\mathrm{ID_2}$, respectively. Throughout this work, we initialize at $r_0=20M$ and we extract the signal at $r_{\rm ext}=300M$. We pick $\sigma=4.0M$ and wave packet frequency $\Omega_0=0.1$, yet tested extensively that our results are independent of these factors.

Impact of plasma on QNMs. When plasma permeates the light ring, BH relaxation is expected to change *in the EM channel*. We indeed find a total suppression of the EM signal at large distances for large $\omega_{\rm p}$. However, we find something more significant, summarized in Fig. 2, which shows the *gravitational* waveform for $\bar{Q}=0.95$ and different plasma frequencies $\omega_{\rm p}^{(\rm c)}$. In absence of plasma, the signal is described by a superposition of gravitational- and EM-led modes, clearly visible (see inset) due to the high coupling Q. A best-fit to the signal shows the presence of two dominant modes, with (complex) frequencies reported in Table I. The plasma suppresses propagation of EM modes when $\omega_{\rm p}$ exceeds the fundamental EM QNM frequency. Our results show that the coupling to GWs also affects the gravitational signal to an important degree. In fact, as apparent in Fig. 2, GWs now carry mostly a single gravitational-led mode (red line), but with a shifted frequency, see Table I. This shift is surprising, and it originates from the coupling between gravity and electromagnetism. The presence of plasma thus affects the QNM frequencies of the gravitational signal.

We confirm these results by frequency-domain calculations (where QNMs are obtained by direct integration with a shooting method) in Table I. Note that we impose purely outgoing boundary conditions at infinity in vacuum, while in the presence of plasma, we consider exponentially decaying EM modes at large distances, to account for

[2]As we will see, the outcome depends on a critical value for $\omega_{\rm p}$ (the fundamental EM QNM), making the density distribution after the barrier ($r>r_{\rm cut}$) or a tenuous plasma before the barrier ($r<r_{\rm cut}$) unimportant for the phenomenology.

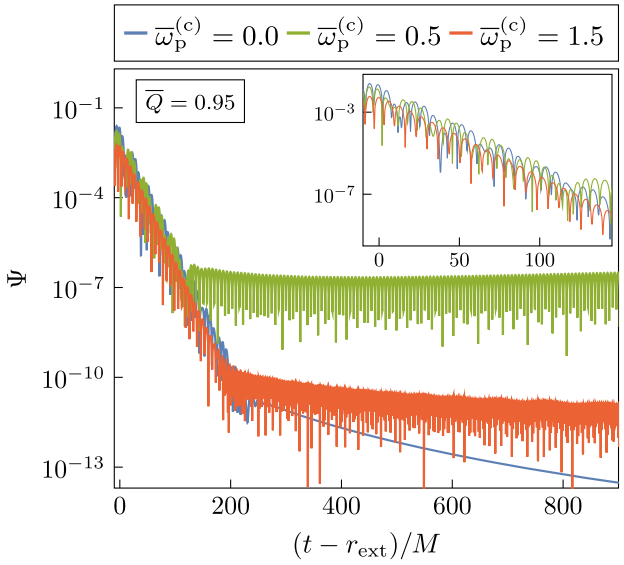

FIG. 2. GWs for $\mathrm{ID_{EM}}$ and $\bar{Q} = 0.95$. For sufficiently dense plasmas (when $\bar{\omega}_{\rm p}^{(c)}$ exceeds the EM QNM frequency), the EM mode is screened. This is apparent in the inset: only one—gravitational-led mode—is present at large plasma frequency. Associated QNM frequencies can be found in Table I. At late times, long-lived modes are excited, in contrast to the usual power-law tail in vacuum. These originate from the quasi-bound states formed in the EM sector and are subsequently imprinted onto the GW signal.

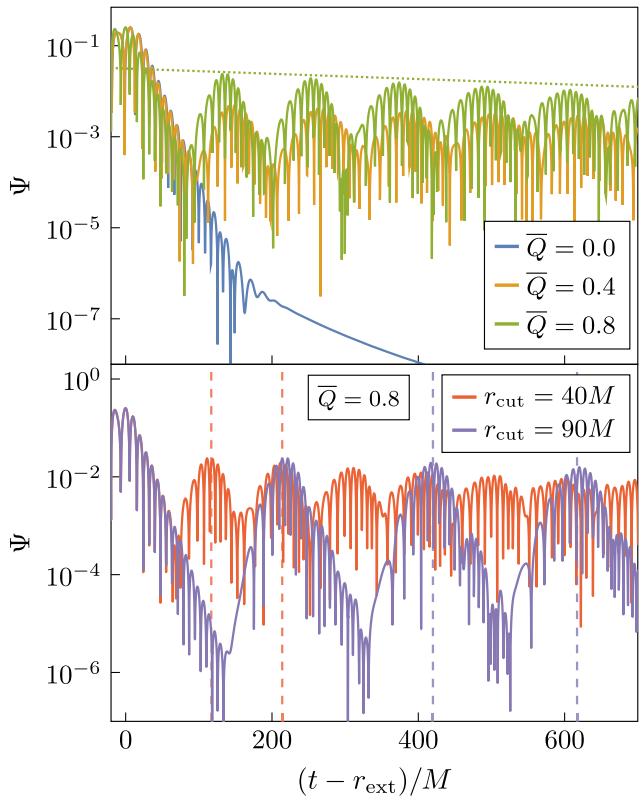

FIG. 3. GW signal generated in the presence of a plasma localized away from the BH. In the top panel $r_{\rm cut} = 40M$; the amplitude of the echoes increases concurrently with the coupling Q. Dotted line indicates the decay rate of the signal, $M\Gamma = -0.00133$, as predicted from (12). Bottom panel illustrates how the echo timescale depends on the position of the plasma barrier. The estimates from (11) are indicated by vertical dashed lines. Both panels are initialized with $\mathrm{ID_g}$ and $\bar{\omega}_{\rm p}^{(c)} = 1.5$.

quasi-bound states (QBS). Clearly, the results from time- and frequency-domain are in good agreement.

On longer timescales, EM QBSs are formed in the presence of plasma (see Supplemental Material [64]) [81,82], which "pollute" the gravitational signal. These are long-lived states which are prevented from leaking to infinity due to the plasma effective mass, and are thus similar to QBS of massive fundamental fields [19]. At late times, we indeed observe a signal ringing at a frequency comparable (yet slightly smaller) than the plasma frequency $\omega_{\rm R} \lesssim \omega_{\rm p}$. As the plasma frequency is increased, the QBSs form at progressively late times, and thus at lower amplitudes, unreachable for observations. This phenomenology is similar to the toy model considered in Ref. [46], but here explored from first principles.

TABLE I. Real (imaginary) part of the fundamental QNM frequencies as calculated from a time- and frequency-domain approach. We consider: (i) no plasma (top row), and we find two modes contributing to the signal and (ii) plasma (bottom row), for which the EM mode is screened and only the gravitational one remains, with a shifted frequency. We obtain similar results in the time-domain, regardless of the chosen ID.

$\bar{Q} = 0.95$	$\bar{\omega}_{\rm QNM}$ (time-domain)	$\bar{\omega}_{\rm QNM}$ (frequency-domain)
$\bar{\omega}_{\rm p}^{(c)} = 0.0$	0.42170 (0.086647)	0.42169 (0.086659)
	0.65475 (0.094609)	0.65476 (0.094605)
$\bar{\omega}_{\rm p}^{(c)} = 1.5$	0.45902 (0.090143)	0.45902 (0.090146)

Propagation: Echoes in waveforms. When the plasma is localized away from the BH, new phenomenology emerges. BH ringdown is associated mostly with light ring physics, hence prompt ringdown is no longer affected [7,83]. However, upon exciting the BH, both EM and GWs travel outward. While GWs travel through the plasma, EM waves are reflected, interacting with the BH again and exciting one more stage of ringdown and corresponding GW "echoes." Such echoes have been found before in the context of (near-) horizon quantum structures [83–86], exotic states of matter in ultracompact/neutron stars [87–89] or modified theories of gravity [90–92] (see [7,93] for reviews). We find them in a general relativity setting.

In the top panel of Fig. 3, we show the GW signal for different BH charge. In contrast to vacuum (where exponential ringdown gives way to a power-law tail), in the presence of plasma prompt ringdown is followed by echoes

of the original burst. For higher BH charge, the reflected EM signal is more strongly coupled, increasing the amplitude of the GW echoes.

The main features of the echoing signal are simple to understand. The time between consecutive echoes can be estimated as (for $r_{\rm cut} \gg r_{\rm LR}$)

$$\Delta t = 2\int_{r_{\rm LR}}^{r_{\rm cut}} \frac{{\rm d}r}{f(r)} \approx 2r_{\rm cut}, \tag{11}$$

This interval is shown by the vertical dashed lines in Fig. 3 and clearly in good agreement with the numerics.

The echo amplitude decays in time, since the BH absorbs part of the reflected waves, and part of the energy is carried to infinity by GWs. The amplitude $A(t)$ of trapped modes in a cavity of length $\sim r_{\rm cut}$ is expected to fall off as

$$A(t) = A_0 e^{-\Gamma t}, \quad \text{with} \quad \Gamma \sim \frac{\mathcal{A}^2}{r_{\rm cut}}, \tag{12}$$

where A_0 is the initial amplitude and $\mathcal{A}^2$ the absorption coefficient of the BH (neglecting losses to GWs at infinity). For simplicity, we take the absorption coefficient of low-frequency monochromatic waves for neutral BHs, given by $\mathcal{A}^2 \sim 256(M\omega_{\rm R})^6/225$ [19,94], where $\omega_{\rm R}$ is the frequency of the trapped EM waves. As the BH absorbs high-frequency modes first, the decay rate decreases over time, asymptoting to a QBS, while the trapped wave packet broadens. Taking $\omega_{\rm R}$ as the highest-frequency peak in the spectrum, we obtain a decay rate (12) in agreement of $\mathcal{O}(1)$ for the first few echoes in Fig. 3. We confirmed that at later times, the high frequency components of the EM field are indeed lost and the decay rate is decreased accordingly. A similar phenomenology can be found for any mechanism that places a BHs in a confining box, e.g. AdS BHs where the AdS radius is much larger than the horizon radius, or Ernst BHs immersed in a magnetic field $B \ll 1/M$ [95].

Conclusions. Plasmas are ubiquitous in the universe, but their impact on our ability to do precision GW physics is poorly understood. We have studied plasma physics in curved spacetime from first principles, capturing their impact on the ringdown of charged BHs. Our results are surprising at first sight. We find an important impact of plasma physics on the *gravitational waves* generated by charged BHs, changing BH spectroscopy to a measurable extend. We see a ringing frequency going up, and the lifetime of the ringdown going down, a behavior that would be important to dissect. We also find that plasmas may trigger measurable echoes in GWs. As the amplitude of these echoes decays slowly, they could be in reach of current or future detectors.

In our work, we focused on values of the plasma frequency $\omega_{\rm p} \sim \mathcal{O}(1/M)$. Note however, that larger values yield similar outcomes. Specifically, a denser plasma present at the light ring causes a greater shift in the gravitational QNM frequency, while a denser plasma localized outside the light ring increases the height of the plasma barrier, making the reflection of photons and thus the echoes, more prominent. Most of our results would also apply to magnetic BHs, which share many similarities with charged BHs in the ringdown phase [96,97]. Finally, as a byproduct, our work introduced a complete framework to describe the behavior of plasmas around charged compact objects in the (non)-relativistic regime. To simplify our analysis, we modeled the background plasma as a nonrelativistic fluid. A complete approach would require consistently evolving the background plasma motion, which is challenging given the large charge-to-mass ratio of electrons (and ions).

Acknowledgments. We thank Paolo Pani for feedback on the manuscript as well as Gregorio Carullo, Marina De Amicis and David Pereñiguez for useful conversations. We acknowledge support by VILLUM Foundation (Grant No. VIL37766) and the DNRF Chair program (Grant No. DNRF162) by the Danish National Research Foundation. V. C. is a Villum Investigator and a DNRF Chair. V. C. acknowledges financial support provided under the European Union's H2020 ERC Advanced Grant "Black holes: gravitational engines of discovery" Grant Agreement No. Gravitas–101052587. This project has received funding from the European Union's Horizon 2020 research and innovation programme under the Marie Sklodowska-Curie Grant Agreements No. 101007855 and No. 101131233.

Views and opinions expressed are however those of the author only and do not necessarily reflect those of the European Union or the European Research Council. Neither the European Union nor the granting authority can be held responsible for them.

[1] B. P. Abbott *et al.* (LIGO Scientific and Virgo Collaborations), Phys. Rev. Lett. **116**, 061102 (2016).
[2] B. P. Abbott *et al.* (LIGO Scientific and Virgo Collaborations), Phys. Rev. X **9**, 031040 (2019).
[3] R. Abbott *et al.* (LIGO Scientific and Virgo Collaborations), Phys. Rev. X **11**, 021053 (2021).
[4] R. Abbott *et al.* (LIGO Scientific, Virgo, and KAGRA Collaborations), Phys. Rev. X **13**, 041039 (2023).
[5] E. Berti *et al.*, Classical Quantum Gravity **32**, 243001 (2015).
[6] L. Barack *et al.*, Classical Quantum Gravity **36**, 143001 (2019).
[7] V. Cardoso and P. Pani, Living Rev. Relativity **22**, 4 (2019).
[8] B. P. Abbott *et al.* (LIGO Scientific and Virgo Collaborations), Phys. Rev. D **100**, 104036 (2019).
[9] R. Abbott *et al.* (LIGO Scientific and Virgo Collaborations), Phys. Rev. D **103**, 122002 (2021).
[10] R. Abbott *et al.* (LIGO Scientific, Virgo, and KAGRA Collaborations), arXiv:2112.06861.
[11] E. Barausse, V. Cardoso, and P. Pani, Phys. Rev. D **89**, 104059 (2014).
[12] V. Cardoso, K. Destounis, F. Duque, R. P. Macedo, and A. Maselli, Phys. Rev. D **105**, L061501 (2022).
[13] V. Cardoso, K. Destounis, F. Duque, R. Panosso Macedo, and A. Maselli, Phys. Rev. Lett. **129**, 241103 (2022).
[14] P. S. Cole, G. Bertone, A. Coogan, D. Gaggero, T. Karydas, B. J. Kavanagh, T. F. M. Spieksma, and G. M. Tomaselli, Nat. Astron. **7**, 943 (2023).
[15] G. Caneva Santoro, S. Roy, R. Vicente, M. Haney, O. J. Piccinni, W. Del Pozzo, and M. Martinez, arXiv:2309.05061.
[16] G. Bertone, D. Hooper, and J. Silk, Phys. Rep. **405**, 279 (2005).
[17] G. Bertone and T. M. P. Tait, Nature (London) **562**, 51 (2018).
[18] G. Bertone *et al.*, SciPost Phys. Core **3**, 007 (2020).
[19] R. Brito, V. Cardoso, and P. Pani, Lect. Notes Phys. **906**, 1 (2015).
[20] D. M. Eardley and W. H. Press, Annu. Rev. Astron. Astrophys. **13**, 381 (1975).
[21] G. W. Gibbons, Commun. Math. Phys. **44**, 245 (1975).
[22] V. Cardoso, C. F. B. Macedo, P. Pani, and V. Ferrari, J. Cosmol. Astropart. Phys. 05 (2016) 054; 04 (2020) E01.
[23] J. A. de Freitas Pacheco, E. Kiritsis, M. Lucca, and J. Silk, Phys. Rev. D **107**, 123525 (2023).
[24] E. Alonso-Monsalve and D. I. Kaiser, Phys. Rev. Lett. **132**, 231402 (2024).
[25] Y. Bai and N. Orlofsky, Phys. Rev. D **101**, 055006 (2020).
[26] K. Kritos and J. Silk, Phys. Rev. D **105**, 063011 (2022).
[27] A. De Rujula, S. L. Glashow, and U. Sarid, Nucl. Phys. **B333**, 173 (1990).
[28] B. Holdom, Phys. Lett. **166B**, 196 (1986).
[29] S. Davidson, S. Hannestad, and G. Raffelt, J. High Energy Phys. 05 (2000) 003.
[30] S. L. Dubovsky, D. S. Gorbunov, and G. I. Rubtsov, JETP Lett. **79**, 1 (2004).
[31] K. Sigurdson, M. Doran, A. Kurylov, R. R. Caldwell, and M. Kamionkowski, Phys. Rev. D **70**, 083501 (2004); **73**, 089903(E) (2006).
[32] H. Gies, J. Jaeckel, and A. Ringwald, Phys. Rev. Lett. **97**, 140402 (2006).
[33] H. Gies, J. Jaeckel, and A. Ringwald, Europhys. Lett. **76**, 794 (2006).
[34] C. Burrage, J. Jaeckel, J. Redondo, and A. Ringwald, J. Cosmol. Astropart. Phys. 11 (2009) 002.
[35] M. Ahlers, Phys. Rev. D **80**, 023513 (2009).
[36] S. D. McDermott, H.-B. Yu, and K. M. Zurek, Phys. Rev. D **83**, 063509 (2011).
[37] A. D. Dolgov, S. L. Dubovsky, G. I. Rubtsov, and I. I. Tkachev, Phys. Rev. D **88**, 117701 (2013).
[38] A. Haas, C. S. Hill, E. Izaguirre, and I. Yavin, Phys. Lett. B **746**, 117 (2015).
[39] M. Khalil, N. Sennett, J. Steinhoff, J. Vines, and A. Buonanno, Phys. Rev. D **98**, 104010 (2018).
[40] A. Caputo, L. Sberna, M. Frias, D. Blas, P. Pani, L. Shao, and W. Yan, Phys. Rev. D **100**, 063515 (2019).
[41] P. K. Gupta, T. F. M. Spieksma, P. T. H. Pang, G. Koekoek, and C. V. D. Broeck, Phys. Rev. D **104**, 063041 (2021).
[42] G. Carullo, D. Laghi, N. K. Johnson-McDaniel, W. Del Pozzo, O. J. C. Dias, M. Godazgar, and J. E. Santos, Phys. Rev. D **105**, 062009 (2022).
[43] D. F. G. Fiorillo and E. Vitagliano, arXiv:2404.07714.
[44] I. Bah and P. Heidmann, Phys. Rev. Lett. **126**, 151101 (2021).
[45] I. Bah and P. Heidmann, J. High Energy Phys. 09 (2021) 128.
[46] V. Cardoso, W.-D. Guo, C. F. B. Macedo, and P. Pani, Mon. Not. R. Astron. Soc. **503**, 563 (2021).
[47] E. W. Leaver, Phys. Rev. D **41**, 2986 (1990).
[48] E. Berti, V. Cardoso, and A. O. Starinets, Classical Quantum Gravity **26**, 163001 (2009).
[49] E. Cannizzaro, A. Caputo, L. Sberna, and P. Pani, Phys. Rev. D **103**, 124018 (2021).
[50] E. Cannizzaro, A. Caputo, L. Sberna, and P. Pani, Phys. Rev. D **104**, 104048 (2021).
[51] A. Einstein, Ann. Math. **40**, 922 (1939).
[52] A. Geralico, F. Pompi, and R. Ruffini, Int. J. Mod. Phys. Conf. Ser. **12**, 146 (2012).
[53] J. C. Feng, S. Chakraborty, and V. Cardoso, Phys. Rev. D **107**, 044050 (2023).
[54] E. Cannizzaro, F. Corelli, and P. Pani, Phys. Rev. D **109**, 023007 (2024).
[55] T. F. M. Spieksma, E. Cannizzaro, T. Ikeda, V. Cardoso, and Y. Chen, Phys. Rev. D **108**, 063013 (2023).
[56] P. J. Armitage and P. Natarajan, Astrophys. J. **634**, 921 (2005).
[57] P. Artymowicz and S. H. Lubow, Astrophys. J. **421**, 651 (1994).
[58] M. Gröbner, W. Ishibashi, S. Tiwari, M. Haney, and P. Jetzer, Astron. Astrophys. **638**, A119 (2020).
[59] B. D. Farris, P. Duffell, A. I. MacFadyen, and Z. Haiman, Mon. Not. R. Astron. Soc. **447**, L80 (2015).
[60] W. Ishibashi and M. Gröbner, Astron. Astrophys. **639**, A108 (2020).
[61] D. J. D'Orazio, Z. Haiman, and A. MacFadyen, Mon. Not. R. Astron. Soc. **436**, 2997 (2013).
[62] H. Canovas, A. Hardy, A. Zurlo, Z. Wahhaj, M. R. Schreiber, A. Vigan, E. Villaver, J. Olofsson, G. Meeus, F. Ménard, C. Caceres, L. A. Cieza, and A. Garufi, Astron. Astrophys. **598**, A43 (2017).
[63] E. Alonso-Monsalve and D. I. Kaiser, Phys. Rev. D **108**, 125010 (2023).

[64] See Supplemental Material at http://link.aps.org/supplemental/10.1103/PhysRevD.110.L021302 for technical details on the perturbation scheme, additional features of the plasma model as well as an extension to the relativistic regime, and convergence tests of our code.
[65] P. Kaw and J. Dawson, Phys. Fluids **13**, 472 (1970).
[66] T. Regge and J. A. Wheeler, Phys. Rev. **108**, 1063 (1957).
[67] F. J. Zerilli, Phys. Rev. D **2**, 2141 (1970).
[68] F. J. Zerilli, Phys. Rev. Lett. **24**, 737 (1970).
[69] F. J. Zerilli, Phys. Rev. D **9**, 860 (1974).
[70] P. Pani, E. Berti, and L. Gualtieri, Phys. Rev. D **88**, 064048 (2013).
[71] J. G. Rosa and S. R. Dolan, Phys. Rev. D **85**, 044043 (2012).
[72] M. Baryakhtar, R. Lasenby, and M. Teo, Phys. Rev. D **96**, 035019 (2017).
[73] V. Moncrief, Phys. Rev. D **10**, 1057 (1974).
[74] V. Moncrief, Phys. Rev. D **9**, 2707 (1974).
[75] V. Moncrief, Phys. Rev. D **12**, 1526 (1975).
[76] A. Zenginoglu and G. Khanna, Phys. Rev. X **1**, 021017 (2011).
[77] W. Krivan, P. Laguna, P. Papadopoulos, and N. Andersson, Phys. Rev. D **56**, 3395 (1997).
[78] E. Pazos-Ávalos and C. O. Lousto, Phys. Rev. D **72**, 084022 (2005).
[79] A. Zenginoglu, G. Khanna, and L. M. Burko, Gen. Relativ. Gravit. **46**, 1672 (2014).
[80] V. Cardoso, F. Duque, and G. Khanna, Phys. Rev. D **103**, L081501 (2021).
[81] G. Lingetti, E. Cannizzaro, and P. Pani, Phys. Rev. D **106**, 024007 (2022).
[82] A. Dima and E. Barausse, Classical Quantum Gravity **37**, 175006 (2020).
[83] V. Cardoso, E. Franzin, and P. Pani, Phys. Rev. Lett. **116**, 171101 (2016); **117**, 089902(E) (2016).
[84] V. Cardoso, S. Hopper, C. F. B. Macedo, C. Palenzuela, and P. Pani, Phys. Rev. D **94**, 084031 (2016).
[85] N. Oshita and N. Afshordi, Phys. Rev. D **99**, 044002 (2019).
[86] Q. Wang, N. Oshita, and N. Afshordi, Phys. Rev. D **101**, 024031 (2020).
[87] V. Ferrari and K. D. Kokkotas, Phys. Rev. D **62**, 107504 (2000).
[88] P. Pani and V. Ferrari, Classical Quantum Gravity **35**, 15LT01 (2018).
[89] L. Buoninfante and A. Mazumdar, Phys. Rev. D **100**, 024031 (2019).
[90] L. Buoninfante, A. Mazumdar, and J. Peng, Phys. Rev. D **100**, 104059 (2019).
[91] A. Delhom, C. F. B. Macedo, G. J. Olmo, and L. C. B. Crispino, Phys. Rev. D **100**, 024016 (2019).
[92] J. Zhang and S.-Y. Zhou, Phys. Rev. D **97**, 081501 (2018).
[93] V. Cardoso and P. Pani, Nat. Astron. **1**, 586 (2017).
[94] A. A. Starobinskil and S. M. Churilov, Sov. Phys. JETP **65**, 1 (1974).
[95] R. Brito, V. Cardoso, and P. Pani, Phys. Rev. D **89**, 104045 (2014).
[96] D. Pereñiguez, Phys. Rev. D **108**, 084046 (2023).
[97] C. Dyson and D. Pereñiguez, Phys. Rev. D **108**, 084064 (2023).